Summer drought and spring frost, but not their interaction, constrain European beech and Silver fir growth in their southern distribution limits

Antonio Gazol[a,b,c], J. Julio Camarero[c,*], Michele Colangelo[c,d], Martín de Luis[e], Edurne Martínez del Castillo[e], Xavier Serra-Maluquer[c]

[a] *Departamento de Biología y Geología, Física y Química Inorgánica, Universidad Rey Juan Carlos, C/Tulipán s/n, 28933, Móstoles, Spain*
[b] *Basque Centre for Climate Change (BC3), Sede Building 1, 48940, Leioa, Spain*
[c] *Instituto Pirenaico de Ecología (IPE-CSIC), Avda. Montaña 1005, 50192, Zaragoza, Spain*
[d] *School of Agricultural, Forest, Food and Environmental Sciences, Univ. Basilicata, Potenza, Italy*
[e] *Department of Geography and Spatial Management, University of Zaragoza, Zaragoza, Spain*

ARTICLE INFO

ABSTRACT

Climate warming has lengthened the growing season by advancing leaf unfolding in many temperate tree species. However, an earlier leaf unfolding increases also the risk of frost damage in spring which may reduce tree radial growth. In equatorward populations of temperate tree species, both late frosts and summer droughts impose two constraints to tree growth, but their effects on growth are understudied. We used a tree-ring network of 71 forests to evaluate the potential influence of late frosts and summer droughts on growth in two tree species that reach their southern distribution limits in north-eastern Spain: the deciduous European beech (*Fagus sylvatica* L.) and the evergreen Silver fir (*Abies alba* Mill). The occurrence of late frost events and summer drought was quantified by using a high-resolution daily temperature and precipitation dataset considering the period 1950–2012. Late frosts were defined as days with average temperature below 0 °C in the site-specific frost-free period, whereas drought was quantified using the 18 month-long August Standardized Precipitation Evapotranspiration Index (SPEI). The growth of European beech and Silver fir was reduced by the occurrence of both late frost events and summer drought. However, we did not find a significant interaction on growth of these two climate extremes. Beech was more negatively impacted by late frosts, whereas Silver fir was more impacted by summer drought. Further studies could use remote-sensing information or in situ phenological records to refine our frost index and better elucidate how late frosts affect growth, whether they interact with drought to constrain growth, and how resilience mechanisms related to post-frost refoliation operate in beech.

1. Introduction

In temperate and Mediterranean biomes, climate has warmed during the last decades (IPCC, 2013) increasing the length of the growing season and advancing leaf unfolding in many tree species (Menzel et al., 2006; Keenan et al., 2014; Fu et al., 2015). While a longer growing season may lead to an earlier leaf unfolding and potentially enhance tree radial growth (Čufar et al., 2015), it might also be a double-edged sword. Advanced leaf-flushing may allow lengthening the growing season through an earlier onset in spring, when water is not limiting (Sánchez-Gómez et al., 2013). Nevertheless, an advanced leaf unfolding increases the risk of frost damage as has been observed in boreal, continental, temperate and mountain forests (Hänninen, 1991; Augspurger, 2009, 2013; Utkina and Rubtsov, 2017;

Vitasse et al., 2018). Current climate projections suggest the increase in the frequency of extreme climate events such late frosts but also droughts and heat weaves (IPCC, 2013), which may negatively impact forest productivity and functioning (Frank et al., 2015).

In the worst scenario, the simultaneous occurrence of spring late frosts together with summer droughts in the same growing season might limit forest productivity by reducing tree radial growth (Rubtsov and Utkina, 2008; Vanoni et al., 2016). This could be the case of several major European tree species dominants in temperate regions such as Silver fir (*Abies alba* Mill., hereafter Silver fir) and European beech (*Fagus sylvatica* L., hereafter beech), which reach their southernmost distribution limit in north-eastern Spain mountains where growth is impaired by low temperatures but also by summer drought (Rozas, 2003; Camarero et al., 2015a, 2015b; Gazol et al., 2015; Martínez del

Castillo et al., 2016; Gazol et al., 2018; Martínez del Castillo et al., 2019a,b). In such transitional regions between temperate and drought-prone Mediterranean conditions, a trade-off may exist between late frost tolerance and summer-drought resistance (Robson et al., 2013). Thus, understanding how temperate tree species as Silver fir and beech respond to the potentially synergic effects of late frosts and summer droughts in their southernmost distribution limit may help to understand the future performance of these species in sight of the climate-change increased air temperature variability.

Late frost damage depends on budburst and leaf-flushing dates and increases with the occurrence of frost events in early spring combined with previous mild temperatures which enhance leaf unfolding (Hänninen, 1991). Frost can damage recently expanded leaves when occurring after leaf-flushing (Augspurger, 2009, 2013; Vitasse et al., 2014a, 2014b), limiting photosynthesis and carbon uptake in spring and subsequently radial growth (Dittmar et al., 2006; Vanoni et al., 2016; Príncipe et al., 2017). Quantifying the effect of late frost damage on radial growth is complicated since phenological records are required to identify how a frost event damages plant tissues. In the absence of such data, the occurrence of frost events in late spring can serve as a proxy to identify the potential impact of late frost events on tree growth (e.g. Vanoni et al., 2016). In this sense, it has been argued that the negative impacts of late frost occurrence on growth may increase polewards (Weigel et al., 2018) and upwards (Vitasse et al., 2018), which suggests that forests located at higher elevation will be the most negatively impacted. However, these assumptions are not supported by recent research. First, European maritime and coastal areas seem to be more exposed to more severe late spring frosts than continental areas (Ma et al., 2019). In addition, climate warming may blur thermal gradients and lead to a more uniform phenology regardless elevation (Chen et al., 2018). Finally, tree species may present enough growth plasticity, or even local genetic adaptations, to override the negative consequences of late frost events on growth (Puchałka et al., 2017).

Whether tree controls on leaf-flushing date is evolutionary linked to the occurrence of late frost events also remains an open debate (Hofmann and Bruelheide, 2015; Körner et al., 2016; Lenz et al., 2016; Vitra et al., 2017), but what is clear is that not all tree species are at the same risk of late frost damage as flushing dates and frost resistance capacity vary across species and populations (Lenz et al., 2016; Bigler and Bugmann, 2018). For example, studies performed in Eastern Europe have identified the existence of different phenological forms in pedunculate oak (*Quercus robur* L.) according to their leaf-flushing behaviours (Rubtsov and Utkina, 2008; Utkina and Rubtsov, 2017). Early-flushing oaks avoid summer drought at a cost of higher frost risk in spring, whilst late-flushing oaks avoid spring frosts but have a shorter growing period. The growth balance of the two phenological forms is similar (Rubtsov and Utkina, 2008). Leaf-out timing of beech occurs earlier than in other co-occurring species, probably because leaf-out is partially controlled by photoperiod in this species, reducing its responsiveness to late-spring frosts (Lenz et al., 2013, 2016; Ma et al., 2019). However, the existence of different phenological forms in relation to leaf flushing dates has been also suggested in the case of beech (Kraj and Sztorc, 2009). In the case of Silver fir, young individuals growing in the shade showed a delayed dormancy break compared to trees growing in the sun which resulted in a reduced impact of late frost damage on leaves and shoots (Spulak and Martincova, 2015). In both tree species, late frost events result in radial growth reductions (Dittmar et al., 2006; Latreille et al., 2017; Príncipe et al., 2017) despite it is expected that the growth of the deciduous beech should be more negatively impacted by spring frost than that of the evergreen Silver fir (Cailleret and Hendrik, 2011; Suvanto et al., 2017). However, warm conditions followed by very low temperatures may also cause needle damage and canopy dieback as trees are exposed to repeated freeze-thaw cycles leading to winter frost drought in conifers (Camarero et al., 2015a).

The occurrence of summer drought is one of the main factors

impairing tree radial growth, reducing productivity and triggering dieback and high mortality rates worldwide (Anderegg et al., 2012). However, tree responses to drought vary according to species specific physiological characteristics and local adaptations (e.g. Gazol et al., 2018). Both, Silver fir and beech are sensitive to summer drought (Camarero et al., 2018), and they have been found to reduce their radial growth because of summer water shortage in their southernmost populations (Gazol et al., 2015; Rozas et al., 2015; Martínez del Castillo et al., 2019a). In north-east Spain, warming accelerated after the 1980s leading to the occurrence of severe droughts (e.g, 1986, 1994–1995, 2005, 2012) causing dieback episodes in both species (Camarero et al., 2015b, 2018; Gazol et al., 2018; Serra-Maluquer et al., 2019). However, the information regarding the occurrence of late frost events in Spain is scarce despite they have been suggested to impact radial growth in Silver fir (Camarero and Gutiérrez, 2017).

Ongoing climate warming may have resulted in a longer growing season due to earlier budburst and leaf unfolding as has been observed in other European regions (e.g. Vitasse et al., 2018). Phenological records also indicate a generalized advancement of leaf unfolding dates across the Iberian Peninsula (Gordo and Sanz, 2010). Advanced leaf unfolding may enhance growth during early spring and avoid the negative consequences of summer drought at the cost of increasing the exposure to late frost damage (Rubtsov and Utkina, 2008; Kraj and Sztorc, 2009; Puchałka et al., 2017). However, there is also a potential risk that late frost and summer drought may occur in the same growing season, thus synergistically reducing radial growth (Vanoni et al., 2016). How these two climatic factors interact and influence tree growth in the southern distribution limits of Silver fir and beech remains an open question. In this study, we aim to advance in our understanding of how these two species respond to late frost, summer drought and their interactions. To this end, we used dendrochronological methods to reconstruct the growth of 33 Silver fir and 38 beech stands during the last 60 years across north-east Spain. Daily climate data at a high spatial resolution were used to calculate late frost and to estimate summer drought. We calculated a frost-index based on daily climatic data as we lacked *in situ* information on the phenology of the two species. We expect that: (i) the radial growth of Silver fir and beech is negatively impacted by the occurrence of both, late frost events and summer drought; (ii) beech shows a higher sensitivity to late frosts as compared to silver fir; and (iii) finally, a significant interaction between late frost events and summer droughts impacting growth and indicating that the simultaneous occurrence of these two climate extremes have a stronger impact than their separate incidence.

2. Material and methods

2.1. Study site and tree species

We studied the radial growth of Silver fir and beech trees in a network of 71 forests located in north east Spain (Fig. 1; Table S1 in Supporting information). Sampled forests were located in mountain areas (Pyrenees, Pre-Pyrenees and the Iberian Range). The mean annual temperature across the study sites was 8.1 °C, ranging from 3.4 °C in the coldest site (Silver fir forest in Panticosa, 1280 m a.s.l) to 12.4 °C in the warmest site (beech forest in Bertiz, 405 m a.s.l). Annual precipitation ranged from 598 mm in the driest site (beech forest in Montsec, 1360 m a.s.l) to 2738 mm in the wettest site (Silver fir forest in Selva de Oza, 1272 m a.s.l). All studied sites are located within the biogeographic distribution range of the two species (San-Miguel-Ayanz et al., 2016).

We chose to study these two species because; (i) their radial growth is sensitive to summer drought and late frost (Dittmar et al., 2006; Gazol et al., 2015, 2018; Rozas et al., 2015); (ii) they often coexist; and (iii) they form their southernmost distribution limits in the studied region. Beech is a deciduous tree widely distributed across European temperate forests, whereas Silver fir is a conifer found in forests with similar climate and soil conditions but mainly restricted to mountain
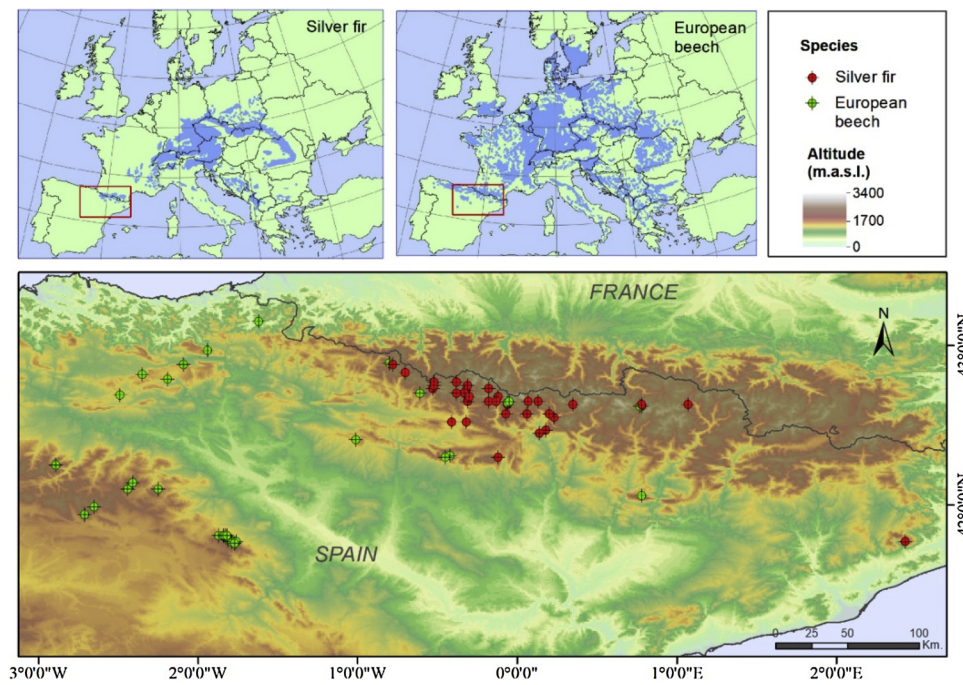
Fig. 1. Silver fir (red dots) and European beech (green dots) forests studied in north eastern Spain. The sampled forests are shown together with altitude. The small maps show the distribution of Silver fir and beech in Europe (http://www.euforgen.org/species/) and the location of the study region in north-eastern Spain. (For interpretation of the references to colour in this figure legend, the reader is referred to the web version of this article.)

areas and cool-wet sites in the study region (Caudullo et al., 2017).

2.2. Tree-ring width data

In each site, a total number ranging from 10 to 40 dominant or co-dominant trees separated by at least 10 m were randomly selected. Trees were cored at 1.3 m height using Pressler increment borers and two cores were extracted per tree. These cores were air dried in the laboratory and mounted on wooden supports for further processing. The samples were sanded with progressively finer sandpapers until tree rings were clearly visible. Ring widths were measured at 0.01 mm resolution using a LINTAB measurement device (Rinntech, Heidelberg, Germany). Visual cross-dating was performed and checked with the program COFECHA (Holmes, 1983).

To quantify the short-term tree growth reductions as a consequence of either late frost events or summer droughts, we calculated the number of individual pointer years at the tree level for the common period for all sites (1950–2012). These individual negative pointer years are annual rings with a substantially smaller width than the n preceding annual rings and reflect growth variability at inter-annual scales that may be associated to extreme climate events, such as frosts and droughts (cf. Schweingruber et al., 1990). Individual pointer years were calculated using normalized growth deviations in a 3-year long window, with a > 0.75 threshold on the so-called Cropper values (Cropper, 1979). When the negative individual pointer years were identified at the tree level, we quantified the percentage of trees displaying negative pointer years for each particular year in each forest. This result in a temporal series of proportion of trees with negative pointer years in each forest (Table S2 Supporting information).

2.3. Climate data

We used two recently developed high resolution gridded datasets (5 × 5 km) of daily precipitation (SPREAD) and maximum and minimum temperatures (STEAD) created for Spain (Serrano-Notivoli et al., 2017a,b, 2019). For each forest, daily time series (1950–2012) for the closest grid point was selected.

To estimate drought severity at each forest, we calculated the Standardized Precipitation and Evapotranspiration Index (hereafter, SPEI) for the period 1950–2012 (Vicente-Serrano et al., 2010). The SPEI

is a measure of drought severity based on temperature and precipitation data and allows comparing drought severity among regions subjected to different climate conditions (Vicente-Serrano et al., 2013). For this reason, we selected SPEI as a measure of drought intensity instead of other metrics such as climatic water balance which are less useful to establish a spatial comparison of drought conditions given the strong climate differences among regions. Negative and positive SPEI values indicate dry and moist conditions, respectively. We calculated 12, 18 and 24-month long summer (June to August) SPEI values for each year, and selected August values because they reflect the maximum cumulative water deficit from the previous to the current growing seasons. In addition, the 18-month long August SPEI was selected because it has a stronger correlation to tree growth than the 12- and 24-month long August SPEIs.

To represent spring late frost events, we created a frost index comparing the averaged minimum daily temperature for the entire study period (1950–2012) with the daily minimum temperature of each particular year (Supporting information, Fig. S1). Ideally, the potential influence of spring frost events on tree growth should be quantified accounting for the phenology of the species. That is, dating the leaf unfolding along the study period to quantify the potential occurrence of frost events affecting recently formed plant tissues and spring growth. However, when this information is not available, using climate data as a surrogate can be a valid approach (Vanoni et al., 2016; Vitasse and Rebetez, 2018). The frost index used here quantifies the magnitude of a frost event occurring in a frost-free period (Vanoni et al., 2016). First, we averaged minimum daily temperatures for the entire study period (1950–2012) considering grid overlapping each study site. In this way we obtained the average minimum temperatures from January to December. Second, we quantified the frost-free period by selecting the dates without average minimum temperatures below zero. To avoid potential bias, i.e. dates with average minimum temperatures above zero followed by temperatures below zero, we selected the last date with average minimum temperatures below zero as the starting date of the frost-free period (following Vanoni et al., 2016). In addition, in those sites where the beginning of the frost-free period started before the beginning of March, we forced it to start by early March assuming that growth stopped during winter in both species. This agrees with observation from nearby areas since leaf unfolding in Silver fir starts in mid-April in France (Cuny et al., 2012), and beech leaf unfolding occurs

between mid-April and early May in Spain (Gordo and Sanz, 2010). Similarly, we forced the frost-free period to end by late August as done by other authors (Vanoni et al., 2016) because 95% of the growth of the species occurs before August (Ellenberg and Leuschner, 2010; Martínez del Castillo et al., 2016). Finally, we used the daily minimum temperature of each year in the frost-free period to quantify the frost index by summing all values below zero for each particular year. Thus, only those days with temperatures below zero in a period which is historically (1950–2012) frost-free can be considered a late or spring frost event according to our method. This was done in each site to account for the potential differences in frost-free period and frost index across sites.

2.4. Statistical analyses

We applied linear mixed-effects models (Pinheiro and Bates, 2000) to study the temporal and spatial variation in the frost index and drought (18 month-long August SPEI). A separate model was created for each variable using the following predictors: calendar year (temporal trend); latitude, longitude and elevation (geographical pattern), averaged mean temperature, and total precipitation (period 1950–2012) and start date of the frost-free period in Julian days (climatic pattern). We included the study site as a random factor (i.e., repeated measures in different years) and the frost index was log-transformed (log (x + 1)) prior to analyses in order to achieve normality assumptions. A first-order autocorrelation structure (AR(1)) was included to account for the potential dependence of the frost index and SPEI in year t of that in year $t-1$ (Zuur et al., 2009).

To identify the set of predictors that better explained the spatio-temporal patterns in frost index and 18 month-long August SPEI we used a multi-model inference approach based on information theory (Burnham and Anderson, 2002). This approach relies on the use of information theory to calculate the relative probability that a given model is more parsimonious than other competing models to explain the response variable. We ranked all potential models according to the second-order Akaike information criterion (AICc). The model showing the lowest AICc value and the largest Akaike weight (w_i, relative probability quantifying if the selected model is the best one) was selected as the best model.

We used different analyses to study the relationship between forest growth and the occurrence of drought and late frost events. First, the Spearman r_s statistic was used to estimate a rank-based measure of association between the annual percentage of trees displaying negative pointer years in each site with the 18 month-long August SPEI and the frost index (Bretz et al., 2010). For each tree species, we studied which factors influenced the correlation between growth (the annual percentage of trees displaying negative pointer years) and drought (18 month-long August SPEI) and between growth and late frosts (frost index). Thus, the above-mentioned correlation coefficients were used as response variables in Generalized Least Squares models (Pinheiro and Bates, 2000). We considered the latitude, longitude, and elevation as well as the maximum, minimum and mean temperature and cumulative precipitation as factors representing the biogeographical gradients of the study region. We also evaluated the second-order polynomial effect of the covariates in order to account for non-linear biogeographic patterns. We ranked all potential models according to the AICc. The model showing the lowest AICc value and the largest w_i was selected as the best model. To quantify the strength of the model, we calculated a pseudo-R^2 (Nagelkerke, 1991).

Finally, to generalize the influence of drought and late frost events on growth for each species, we applied Linear Mixed-Effects models (LME; Pinheiro and Bates, 2000). Separate models were constructed for each species, using the yearly percentage of negative pointer years in each forest as response variables and the frost index, the 18 month-long August SPEI and their interaction as explanatory variables. We included the study site as a random factor since repeated measures (i.e., growth

in different years) were obtained for each forest. The percentage of negative pointer years and the frost index were log-transformed (log (x +1)) prior to analyses in order to achieve normality assumptions. A first-order autocorrelation structure (AR(1)) was included to account for the potential dependence of the percentage of negative pointer years in year t of that in year $t-1$ (Zuur et al., 2009). A graphical examination of the model showed a heterogeneous distribution of residuals (Zuur et al., 2010), and thus a constant variance function structure was included to account for the variation in the occurrence of negative pointer years across sites (Zuur et al., 2009). To identify the set of predictors that better explained the occurrence of negative pointer years in the LMEs (i.e. frost-index, 18 month-long August SPEI and their interaction) we used a multi-model inference approach based on information theory (Burnham and Anderson, 2002). The model showing the lowest AICc value and the largest w_i was selected as the most parsimonious model. To quantify the strength of the LMEs, we calculated marginal (R^2 which accounts for fixed factors) and conditional (R^2 which accounts for fixed plus random factors) R^2 values (Nakagawa and Schielzeth, 2013).

All statistical analyses were performed in the R statistical environment (R Development Core Team, 2017). The dplR package was used to manage tree-ring width series, detrend them and calculate the chronologies (Bunn et al., 2016). To detect individual pointer years we used the function pointer.norm of the package 'pointRes' (van der Maaten-Theunissen et al., 2015). The lme function of the 'nlme' package was used to fit the Linear Mixed-Effects models (Pinheiro et al., 2014). The 'MuMIn' package was used to perform the multi-model selection and calculate pseudo-R^2 (Barton, 2012).

3. Results

The percentage of trees displaying negative pointer years varied between species. Silver fir presented a large percentage of trees (> 50%) showing a negative pointer year in 1965, 1984 and 1986 (Fig. 2). In the case of beech negative pointer years were abundant in 1968, 1994–1995, 1999, 2003, and 2010. Dry conditions (negative 18 month-long August SPEI values) prevailed across sites in years 1986,
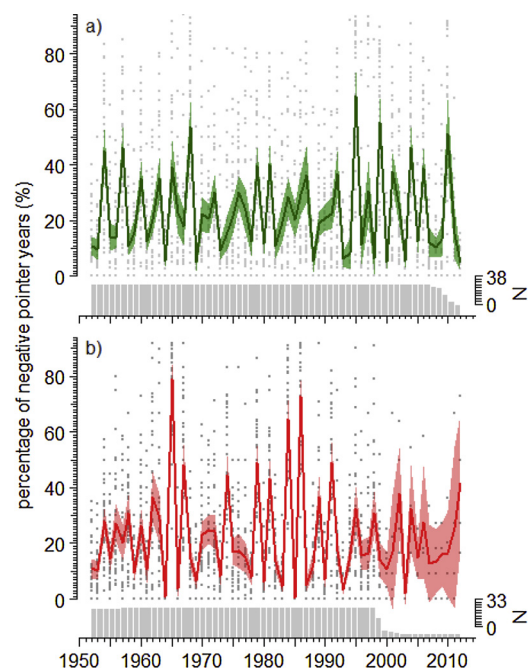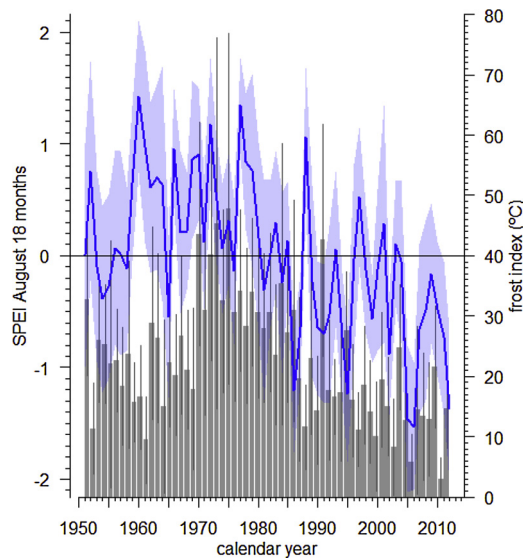

Fig. 2. Mean percentage of trees displaying negative pointer years in the two tree species (a, beech; b, Silver fir). Shaded areas represent standard errors. Points indicate site values. Grey bars (secondary y-axis) represent the number of sites (N) with observations for each particular year.

Fig. 3. Variability of the 18-month long August SPEI drought index (blue line is the mean) and the frost index (grey bars with higher values indicating higher frost incidence) during the study period (1950–2012). The shaded blue areas represent the standard error for the SPEI mean, and the vertical lines the standard deviation for the frost index. (For interpretation of the references to colour in this figure legend, the reader is referred to the web version of this article.)

Fig. 4. Spatial variation of selected climate variables across the study area in north-eastern Spain: (a), De Martonne aridity index (De Martonne, 1926); (b), April minimum temperatures; (c), De Martonne aridity index; and (d), frost index. The symbols size is proportional to: a) mean percentage of trees displaying negative pointer years; b) beginning of the frost free period in Julian days (DOY); c) correlations between the percentage of trees displaying negative pointer years and 18 month-long August SPEI; and d) correlations between the percentage of trees displaying negative pointer years and the frost index. Red and green symbols indicate the sampled Silver fir and beech forests, respectively. (For interpretation of the references to colour in this figure legend, the reader is referred to the web version of this article.)

1994–1995, and 2005, whereas frost incidence (high values of the frost index) was common in 1975, 1984 and 1991. A marked trend in SPEI towards more negative values (dryer conditions) was observed, whilst frost incidence peaked in the 70s and decreased after that (Fig. 3). Along this, the results of the LME showed that both, SPEI and frost index has decreased significantly over the last decades (Table 1).
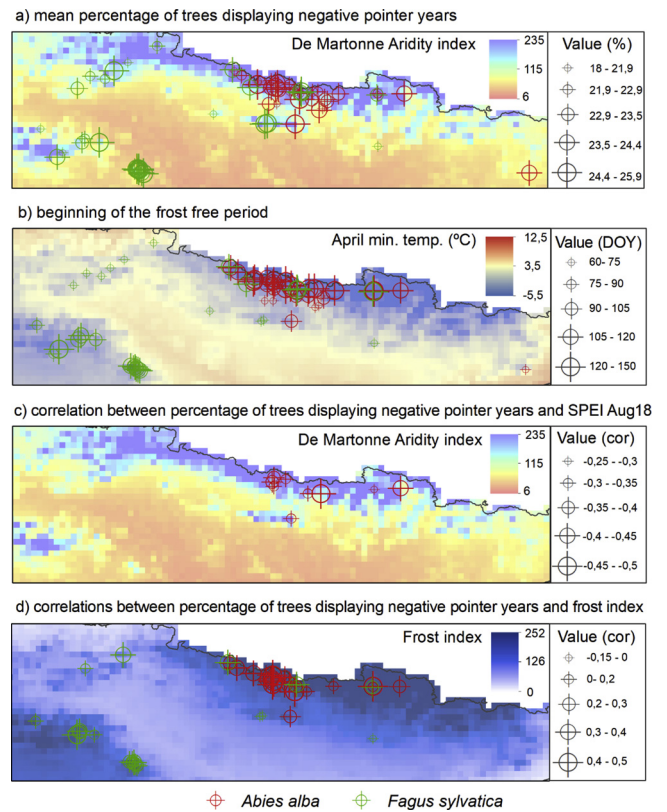
The frost index increased with elevation, and decreased with latitude, mean annual temperature and the start of the frost free period (Table 1). The start of the frost-free period (Fig. 4) was positively related with site longitude ($r = 0.33$; $p < 0.01$), elevation ($r = 0.47$, $p < 0.01$) and annual precipitation ($r = 0.58$, $p < 0.01$), and it was negatively related with the increase in annual temperature ($r = -0.94$, $p < 0.01$). When separated for tree species, the start of the frost-free period was strongly linked to elevation in beech ($r = 0.83$, $p < 0.01$), whereas in the case of Silver fir it was related to latitude ($r = 0.49$, $p < 0.01$). Across sites, beech forests from warm-dry sites from the Iberian Range (e.g. M14FS, 1440 m a.s.l; Fig. 4; see also Table S1) showed the highest proportion of negative pointer years (25.7%), whereas in the case of Silver fir this was observed in the central Pyrenean site "FAAA" located at 918 m a.s.l.

We found nine Silver fir forests (27%) showing a significant negative correlation between the percentage of trees displaying negative pointer years and the SPEI. Similarly, twelve beech stands (32%) plus twelve silver fir stands (36%) showed a significant positive relationship between the frequency of negative pointer years and frost index (Table 2, Fig. 4). The correlation between negative pointer years occurrence and 18 month-long August SPEI decreased with longitude and

increased with elevation (Table 3). Conversely, the correlation between negative pointer years occurrence and frost index increased with latitude and showed a quadratic relationship with site mean average temperature (Table 3).

The selected linear mixed-effect model indicated the existence of a positive relationship between the occurrence of negative pointer years and the 18 month-long August SPEI for both species (Table 4), confirming that growth was reduced by dry conditions during and before the growing season (Fig. 5). The strength of the association between drought (SPEI) and the occurrence of negative pointer years was higher in the case of Silver fir than in the case of beech (Table 4; Fig. 5). Similarly, the two tree species showed a positive relationship between the occurrence of negative pointer years and the frost index, indicating that spring late frosts reduced radial growth. However, this effect was slightly stronger in the case of beech than in Silver fir (Table 4, Fig. 5).

Table 1

Results of the linear mixed-effects models selected to study the spatiotemporal patterns in drought intensity (18 month-long August SPEI) and frost index. For each variable, the covariates included in the model are displayed (t-statistic). These covariates are: elevation (m a.s.l), latitude (decimal degrees), mean annual temperature (T Med; in ºC) and beginning of the frost-free period (ffp). The Akaike weight of the model (w_i) and the marginal R^2 values (conditional R^2 values are indicated between parenthesis) are displayed. Significant values are indicated with asterisks (** $p < 0.01$).

	Year	Elevation	Latitude	T Med	ffp	w_i	R^2
SPEI	−15.49**	–	–	–	–	27%	0.15 (0.15)
Frost index	−16.78**	3.10**	−5.47**	−9.05**	−9.71**	22%	0.17 (0.21)

Table 2

Spearman correlation coefficients (r_s) calculated by relating the occurrence of negative pointer years in radial growth and the 18-month long August SPEI and frost-index.

Tree species	Site	r_s August SPEI	p	r_s frost-index	p
Silver fir	ABAA	−0.2	0.174	0.355	0.013
	ASAA	−0.135	0.359	0.369	0.01
	CAAA	−0.306	0.034	0.432	0.002
	CHAA	−0.229	0.089	0.426	0.001
	COA	−0.162	0.277	0.43	0.003
	MAA	−0.404	0.005	0.271	0.065
	GAAA	−0.149	0.251	0.264	0.04
	GUAA	−0.311	0.034	0.269	0.067
	IAAA	−0.363	0.011	0.414	0.003
	LIAA	−0.36	0.013	0.331	0.023
	LOAA	−0.282	0.055	0.321	0.028
	ORAA	−0.302	0.037	0.179	0.223
	PAAA	−0.332	0.021	0.228	0.119
	SNAA	−0.436	0.002	−0.06	0.684
	SOAA	−0.212	0.152	0.302	0.039
	VIAA	−0.279	0.048	0.405	0.003
	YEAA	−0.243	0.092	0.4	0.004
Beech	COFS	−0.044	0.734	0.275	0.032
	AIFS	−0.067	0.608	0.501	0.000
	DIFS	−0.1	0.446	0.468	0.000
	EAFS	−0.126	0.332	0.33	0.009
	GAFS	−0.048	0.716	0.351	0.006
	L1FS	0.042	0.749	0.366	0.004
	L2FFs	0.004	0.975	0.299	0.021
	M4FS	−0.063	0.636	0.278	0.034
	M5FS	−0.112	0.403	0.278	0.034
	M10F	−0.008	0.953	0.367	0.004
	M17F	−0.083	0.534	0.285	0.030
	OR3F	0.013	0.924	0.319	0.014

The selected model in the case of Silver fir accounted for 5% of the variation in the occurrence of negative pointer years (Table 4). Similarly, in the case of beech the model accounted for 9% of the variation. The effect of late frosts on growth was twice as important as the drought effect in beech. The interaction between the frost index and the August SPEI was not significant in the selected model.

4. Discussion

Our results support the hypothesis that the radial growth of Silver fir and beech is negatively impacted by the occurrence of both, late frost events and summer drought near their southernmost distribution limits. The occurrence of negative pointer years in the two species increases with the increase in frost index and decreases with the decrease in 18 month-long August SPEI. We found that the radial growth of beech was particularly susceptible to late frost, thus partially supporting our second hypothesis. However, the lack of a significant interaction between frost index and SPEI do not support the hypothesis that the simultaneous occurrence of these two climate extremes more strongly impacted on growth than their separate incidence. These results shall be interpreted with caution as they can be contingent on the definition of the frost index. Here, we defined the frost-free period as the period without late frost events based on daily climate conditions solely, and thus we lacked information on when leaf unfolding occurs in the

Table 4

Statistics of the selected linear-mixed effects model fitted to the occurrence of negative pointer years as a function of the 18 month-long August SPEI, the frost index and their interaction. The ΔAICc, Akaike weight (w_i) and pseudo-R^2 of the selected models are shown. The two values in the last column indicate the marginal and conditional (between parentheses) R^2 values, respectively.

Tree species	Variable	t value	p	ΔAICc	w_i	R^2
Silver fir	SPEI	−6.73	< 0.01	1.11	0.64	0.04 (0.05)
	Frost index	5.74	< 0.01			
	Interaction	–	–			
Beech	SPEI	−3.89	< 0.01	0.22	0.53	0.04 (0.09)
	Frost index	7.39	< 0.01			
	Interaction	–	–			
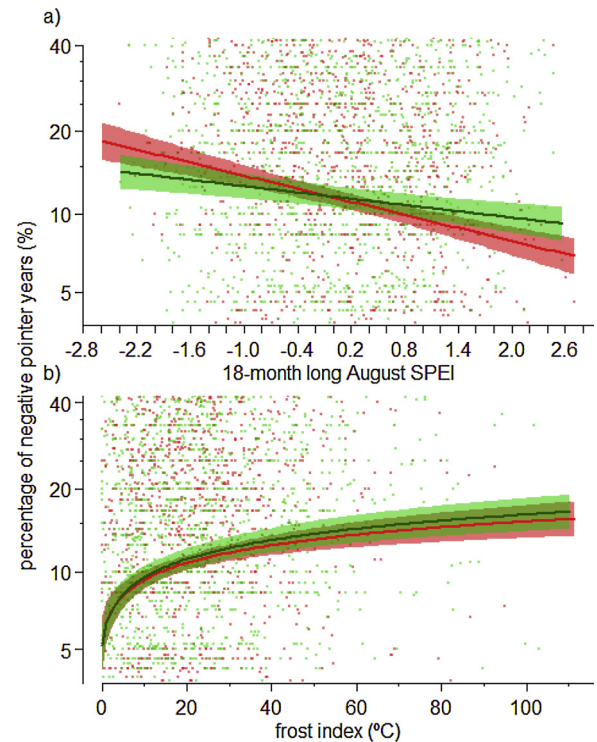
Fig. 5. Effects of drought (18-month long August SPEI) and frost index (ºC) on the percentage of negative pointer years in Silver fir (red lines and symbols) and beech (green lines and symbols) according to the selected Linear Mixed-Effect models (see Table 4). (For interpretation of the references to colour in this figure legend, the reader is referred to the web version of this article.)

sampled sites and during the study period. Further studies considering a more mechanistic definition of the frost-free period and the beginning of the leaf unfolding season using *in situ* phenological records or satellite-derived phenological surrogates may test if the frost index is a valid approach to quantify the occurrence of late frost events and their impact on growth.

We found a significant increase in the occurrence of negative pointer years with the decrease in the 18 month-long August SPEI indicating the sensitivity of the radial growth of Silver fir to summer

Table 3

Results of the linear models selected to study the spatial patterns in the correlations between negative pointer years, drought intensity (18 month-long August SPEI) and frost index. For each variable, the covariates included in the model are displayed (*t* statistic). The Akaike weight of the model (w_i) and the pseudo-R^2 are displayed. TMed is the mean temperature.

	Elevation	longitude	Latitude	T Med	TMed^2	w_i	Pseudo-R^2
r_s SPEI	3.34**	−6.38**	–	–	–	18%	0.38
r_s frost-index	–	–	2.13*	3.82**	−4.37**	15%	0.33

drought in agreement with previous studies (Camarero et al., 2015a,b; Gazol et al., 2015, 2018; Serra-Maluquer et al., 2019). The responsiveness of Silver fir to drought could explain the occurrence of dieback episodes on Pyrenean forests which has been observed from the 1980s onwards (Gazol et al., 2015). The post-1970s warming trends and the occurrence of severe droughts have been identified as important factors contributing to this decline (Sangüesa-Barreda et al., 2015). In particular, the severe 1985–1986 drought (see Figs. 3 and 4) has been identified as the starting point for this declining trend (Camarero et al., 2018; Camarero et al., 2011), which was intensified by successive droughts such as those occurring in 2005 and 2012 (Camarero et al., 2015b). Nevertheless, the 1986 spring was very cold in some sites where spring frosts occurred (Fig. 3), so the potential interaction between drought and cold stress should be further investigated in those sites. Regarding beech, several studies have also demonstrated that its growth is impaired by summer drought (Rozas, 2003; Rozas et al., 2015; Serra-Maluquer et al., 2019). A recent study considering several populations across north-eastern Spain, suggests that the radial growth of beech is decreasing as a consequence of global warming (Serra-Maluquer et al., 2019). We found that drought intensity has increased in the study region during the last decades (Table 2), and that this has reduced the radial growth in beech as confirmed by the linear mixed-effect models. However, the site to site analyses showed no significant influence of SPEI on the occurrence of severe growth reductions in beech. Thus, our results suggest that the radial growth of Silver fir is more sensitive to summer drought than the growth of beech near their southern distribution limits. This situation can be related to the fact that some studied Silver fir forests are situated in regions with dieback episodes occurring during the last decades (e.g. Camarero et al., 2018; Gazol et al., 2015), whilst few beech stands showed symptoms associated to drought-induced dieback (Camarero et al., 2018).

We found that the occurrence of negative pointer years in Silver fir and beech was positively related to the frost index. A similar number of forests of the two species (Table 2) showed an impact of the frost index on the occurrence of negative pointer years. However, the fitted models suggest that beech growth is slightly more impacted by late frosts than Silver fir growth (Table 3; Fig. 4). Latreille et al. (2017) found a marked sensitivity of Silver fir growth to the occurrence of summer drought and frost along two altitudinal gradients in south-eastern France. Cailleret and Hendrik (2011) found a higher sensitivity of beech to both, summer drought and late frost, along a wide altitudinal and climatic gradient in southern France. In our study, most of the studied Silver fir stands are mountain forests found at intermediate to high elevations (from 918 to 2008 m), whereas beech forests display a greater altitudinal gradient (from 405 to 1850 m) encompassing mountain and lowland forests. This is probably the reason for the strong linkage between the start of the frost-free period and site elevation in the case of beech, whereas in Silver fir it was mainly related with site latitude. These differences together with the widespread decline of silver fir in the region as a consequence of drought could explain the higher sensitivity to drought of Silver fir, and the marked growth responsiveness to frost in beech.

The occurrence of late frost events can impact tree growth negatively due to two mechanisms: frost damage in the bursting buds and expanding leaves and frost-induced xylem embolism (Fernández-Pérez et al., 2018). However, the freezing-tolerance of the study species in winter is much higher that the negative temperatures reached during spring frosts (Sakai and Larcher, 1987). In this sense, it is unlikely that frost-induced xylem embolism (e.g. Camarero et al., 2015a) can be impairing growth in the selected sites. Most likely, negative impacts of frost on drought may occur as a consequence of the death of young leaves just after flushing (Augspurger, 2009). This will explain why the deciduous beech is more sensitive to late frost events than the evergreen Silver fir. However, further research is required to disentangle the mechanisms by which late frost events can reduce growth of these species. Moreover, it is also plausible to think that not all late frost events translate into growth reductions (Puchałka et al., 2016, 2017) as

favourable growing seasons can mitigate its impacts. Thus, post-frost resilience mechanisms should also have to be considered including a higher photosynthesis rate and lifespan of second-cohort leaves or an enhanced autumn bud growth, changes which allow compensating for spring frost damage in beech saplings (Zohner et al., 2019). In addition, beech shows a conservative phenology as compared with other tree species (e.g. *Acer* spp.), which leaf out earlier and are more affected by spring frosts (Hufkens et al., 2012; Ma et al., 2019).

Evaluating long-term late frost damage on tree performance is challenging as it requires reconstructing phenology and local climate conditions (Augspurger, 2013). This is particularly important mostly considering that different phenological forms of the same species can coexist even within a region (Rubtstov and Utkina, 2008; Kraj and Sztorc, 2009; Utkina and Rubtsov, 2017), and that trees can have local adaptations to tolerate late frost events or to recover after them (Puchałka et al., 2017). In this study, we followed a conservative definition of late frost events by considering that the start of the frost-free period in each site was fixed during the study period (1950–2012), and by considering only the frosts that occurred during this period. The frost-free period started right after early March in only six beech forests with mean annual temperatures above 10 °C. Conversely, in eleven Silver fir sites and four beech sites the frost-free period started after early May, and those sites had mean annual temperatures below 6 °C. Probably because of global warming, the occurrence of late frost events, as defined in this study, has decrease in the study region (Table 2). However, it is also plausible to think that the phenology of the tree species is changing (Gordo and Sanz, 2010; Vitasse et al., 2014b). Thus, our conservative definition of frost-index could be reformulated considering other factors as the photoperiod (Körner et al., 2016). In addition, better assessments of frost impacts based on remote-sensing or digital camera data may help to advance in this topic (Richardson et al., 2018).

To conclude, beech and Silver fir growth was reduced by both late frosts and summer droughts, but not by their interaction. Beech growth was mainly impacted by late frosts, whereas Silver fir growth was more constrained by dry summers despite it also responded to late frost. Further studies should use phenological information to pinpoint frost effects on growth and, and also investigate resilience patterns related to post-frost refoliation.

Appendix A. Supplementary data

Supplementary material related to this article can be found, in the online version, at doi:https://doi.org/10.1016/j.agrformet.2019.107695.

References

Anderegg, W.R.L., Kane, J.M., Anderegg, L.D.L., 2012. Consequences of widespread tree mortality triggered by drought and temperature stress. Nat. Clim. 30–36 Ch. 3.

Augspurger, C.K., 2009. Spring 2007 warmth and frost: phenology, damage and refoliation in a temperate deciduous forest. Funct. Ecol. 23, 1031–1039.

Augspurger, C.K., 2013. Reconstructing patterns of temperature, phenology, and frost damage over 124 years: spring damage risk is increasing. Ecology 94, 41–50.

Barton, K., 2012. MuMIn: Multi-Model Inference. (R Package Version 1.7.7). Available at. http://CRAN.R-project.org/package=MuMIn.

Bigler, C., Bugmann, H., 2018. Climate-induced shifts in leaf unfolding and frost risk of European trees and shrubs. Sci. Rep. 8, 9865.

Bretz, F., Hothorn, T., Westfall, P., 2010. Multiple Comparisons Using R. Chapman & Hall/CRC Press, Boca Raton, USA.

Bunn, A., Korpela, M., Biondi, F., Campelo, F., Mérian, P., Qeadan, F., et al., 2016. dplR: Dendrochronology Program Library in R. R Package Version 1.6.4. https://CRAN.R-project.org/package=dplR.

Burnham, K.P., Anderson, D.R., 2002. Model Selection and Multimodel Inference: A Practical Information-theoretic Approach. Springer, New York.

Cailleret, M., Hendrik, D., 2011. Effects of climate on diameter growth of co-occurring *Fagus sylvatica* and *Abies alba* along an altitudinal gradient. Trees-Struct. Funct. 25, 265–276.

Camarero, J.J., Bigler, C., Linares, J.C., Gil-Pelegrín, E., 2011. Synergistic effects of past historical logging and drought on the decline of Pyrenean silver fir forests. For. Ecol. Manag. 262, 759–769.

Camarero, J.J., Gazol, A., Sancho-Benages, S., Sangüesa-Barreda, G., 2015a. Know your limits? Climate extremes impact the range of Scots pine in unexpected places. Ann. Bot. 116, 917–927.

Camarero, J.J., Gazol, A., Sangüesa-Barreda, G., Oliva, J., Vicente-Serrano, S.M., 2015b. To die or not to die: early-warning signals of dieback in response to a severe drought. J. Ecol. 103, 44–57.

Camarero, J.J., Gazol, A., Sangüesa-Barreda, G., Cantero, A., Sánchez-Salguero, R., Sánchez-Miranda, A., et al., 2018. Forest growth responses to drought at short- and long-term scales in Spain: squeezing the stress memory from tree rings. Front. Ecol. Evol. 6, 9. https://doi.org/10.3389/fevo.2018.00009.

Camarero, J.J., Gutiérrez, E., 2017. Wood density of silver fir reflects drought and cold stress across climatic and biogeographic gradients. Dendrochronologia 45, 101–112.

Caudullo, G., Welk, E., San-Miguel-Ayanz, J., 2017. Chorological maps for the main European woody species. Data Brief 12, 662–666.

Chen, L., Huang, J.-G., Ma, Q., Hänninen, H., Rossi, S., Piao, S., Bergeron, Y., 2018. Spring phenology at different altitudes is becoming more uniform under global warming in Europe. Glob. Change Biol. 24, 3969–3975.

Cropper, J.P., 1979. Tree-ring skeleton plotting by computer. Tree-Ring Bull. 39, 47–59.

Čufar, K., de Luis, M., Prislan, P., Gričar, J., Črepinšek, Z., Merela, M., Kajfež-Bogataj, L., 2015. Do variations in leaf phenology affect radial growth variations in *Fagus sylvatica*? Int. J. Biometeorol. 59, 1127–21132.

Cuny, H.E., Rathgeber, C.B.K., Lebourgeois, F., Fortin, M., Fournier, M., 2012. Life strategies in intra-annual dynamics of wood formation: example of three conifer species in a temperate forest in north-east France. Tree Physiol. 32, 612–625.

De Martonne, E., 1926. Une nouvelle fonction climatologique: L'indice d'aridité. La Meteorol. 449–458.

Dittmar, C., Fricke, W., Elling, W., 2006. Impact of late frost events on radial growth of common beech (*Fagus sylvatica* L.) in Southern Germany. Eur. J. For. Res. 125, 249–259.

Ellenberg, H., Leuschner, C., 2010. Vegetation Mitteleuropas mit den Alpen. Eugen Ulmer, Stuttgart, Germany.

Fernández-Pérez, L., Villar-Salvador, P., Martínez-Vilalta, J., Toca, A., Zavala, M.A., 2018. Distribution of pines in the Iberian Peninsula agrees with species differences in foliage frost tolerance, not with vulnerability to freezing-induced xylem embolism. Tree Physiol. 38, 507–516.

Frank, D., Reichstein, M., Bahn, M., Thonicke, K., Mahecha, M.D., et al., 2015. Effects of climate extremes on the terrestrial carbon cycle: concepts, processes and potential future impacts. Glob. Change Biol. 21, 2861–2880.

Fu, Y.H., Zhao, H., Piao, S., Peaucelle, M., Peng, S., Zhou, G., Ciais, P., Huang, M., Janssens, I., et al., 2015. Declining global warming effects on the phenology of spring leaf unfolding. Nature 526, 104–107.

Gazol, A., Camarero, J.J., Gutiérrez, E., Popa, I., Andreu-Hayles, L., Motta, R., et al., 2015. Distinct effects of climate warming on populations of silver fir (*Abies alba*) across Europe. J. Biogeogr. 42, 1150–1162.

Gazol, A., Camarero, J.J., Vicente-Serrano, S.M., Sánchez-Salguero, R., Gutiérrez, E., De Luis, M., et al., 2018. Forest resilience to drought varies across biomes. Glob. Change Biol. 24, 2143–2158.

Gordo, O., Sanz, J.J., 2010. Impact of climate change on plant phenology in Mediterranean ecosystems. Glob. Change Biol. 16, 1082–1106.

Hänninen, H., 1991. Does climatic warming increase the risk of frost damage in northern trees? Plant Cell Environ. 14, 449–454. https://doi.org/10.1111/j.1365-3040.1991.tb01514.x.

Hofmann, M., Bruelheide, H., 2015. Frost hardiness of tree species is independent of phenology and macroclimatic conditions. J. Biosci. 40, 147–157.

Holmes, R.L., 1983. Computer-assisted quality control in tree-ring dating and measurement. Tree-Ring Bull. 43, 69–78.

Hufkens, K., Friedl, M.A., Keenan, T.F., Sonnentag, O., Bailey, A., O'Keefe, J., Richardson, A.D., 2012. Ecological impacts of a widespread frost event following early spring leaf-out. Glob. Change Biol. 18, 2365–2377.

IPCC, 2013. Summary for policymakers. In: Stocker, T.F., Qin, D., Plattner, G.-K., Tignor, M., Allen, S.K., Boschung, J., Nauels, A., Xia, Y., Bex, V., Midgley, P.M. (Eds.), Climate Change 2013: The Physical Science Basis. Contribution of Working Group I to the Fifth Assessment Report of the Intergovernmental Panel on Climate Change. Cambridge University Press, Cambridge, UK, pp. 3–29.

Keenan, T.F., Gray, J., Friedl, M.A., et al., 2014. Net carbon uptake has increased through warming-induced changes in temperate forest phenology. Nat. Clim. 598–604 Ch. 4.

Körner, C., Basler, D., Hoch, G., Kollas, C., Lenz, A., Randin, C., Vitasse, Y., Zimmermann, N.E., 2016. Where, why and how? Explaining the low temperature range limits of temperate tree species. J. Ecol. 104, 1076–1088.

Kraj, W., Sztorc, A., 2009. Genetic structure and variability of phenological forms in the European beech (*Fagus sylvatica* L.). Ann. For. Sci. 66, 203.

Latreille, A., Davi, H., Huard, F., Pichot, C., 2017. Variability of the climate-radial growth relationship among *Abies alba* trees and populations along altitudinal gradients. For. Ecol. Manag. 396, 150–159.

Lenz, A., Hoch, G., Vitasse, Y., Korner, C., 2013. European deciduous trees exhibit similar safety margins against damage by spring freeze events along elevational gradients. New Phytol. 200, 1166–1175.

Lenz, A., Hoch, G., Körner, C., Vitasse, Y., 2016. Convergence of leaf-out timing towards

minimum risk of freezing damage in temperate trees. Funct. Ecol. 30, 1480–1490.

Ma, Q., Huang, J.-G., Hänninen, H., Berninger, F., 2019. Divergent trends in the risk of spring frost damage to trees in Europe with recent warming. Glob. Change Biol. 25, 351–360.

Martínez del Castillo, E., Longares, L.A., Gričar, J., Prislan, P., Gil-Pelegrín, E., Čufar, K., De Luis, M., 2016. Living on the edge: contrasted wood-formation dynamics in *Fagus sylvatica* and *Pinus sylvestris* under Mediterranean conditions. Front. Plant Sci. 7, 370.

Martínez del Castillo, E., Longares, L.A., Serrano-Notivoli, R., Sass-Klaassen, U.G.W., De Luis, M., 2019a. Spatial patterns of climate-growth relationships across species distribution as a forest management tool in Moncayo Natural Park (Spain). Eur. J. For. Res. 138, 299–312. https://doi.org/10.1007/s10342-019-01169-3.

Martínez del Castillo, E., Longares, L.A., Serrano-Notivoli, R., De Luis, M., 2019b. Modeling tree-growth: assessing climate suitability of temperate forests growing in Moncayo Natural Park (Spain). For. Ecol. Manag. 435, 128–137.

Menzel, A., Sparks, T.H., Estrella, N., Koch, E., Aasa, A., Ahas, R., et al., 2006. European phenological response to climate change matches the warming pattern. Glob. Change Biol. 12, 1969–1976.

Nagelkerke, N.J.D., 1991. A note on a general definition of the coefficient of determination. Biometrika 78, 691–692.

Nakagawa, S., Schielzeth, H., 2013. A general and simple method for obtaining R^2 from generalized linear mixed-effects models. Methods Ecol. Evol. 4, 133–142.

Pinheiro, J.C., Bates, D.M., 2000. Mixed-Effects Models in S and S-PLUS. Springer-Verlag, New York.

Pinheiro, J., Bates, D., DebRoy, S., Sarkar, D., 2014. nlme: Linear and Nonlinear Mixed Effects Models. R Package Version 3.1-117.

Príncipe, A., van der Maaten, E., van der Maaten-Theunissen, M., Struwe, T., Wilmking, M., Kreyling, J., 2017. Low resistance but high resilience in growth of a major deciduous forest tree (*Fagus sylvatica* L.) in response to late spring frost in southern Germany. Trees-Struct. Funct. 31, 743–751.

Puchałka, R., Koprowski, M., Przybylak, J., Przybylak, R., Dąbrowski, H.P., 2016. Did the late spring frost in 2007 and 2011 affect tree-ring width and earlywood vessel size in Pedunculate oak (*Quercus robur*) in northern Poland? Int. J. Biometeorol. 60, 1143–1150.

Puchałka, R., Koprowski, M., Gričar, J., Przybylak, R., 2017. Does tree-ring formation follow leaf phenology in Pedunculate oak (*Quercus robur* L.)? Eur. J. For. Res. 136, 259–268.

R Core Team, 2017. R: A Language and Environment for Statistical Computing. R Foundation for Statistical Computing, Vienna, Austria.

Richardson, A.D., Hufkens, K., Milliman, T., Aubrecht, D.M., Chen, M., Gray, J.M., Johnston, M.R., Keenan, T.F., Klosterman, S.T., Kosmala, M., Melaas, E.K., Friedl, M.A., Frolking, S., 2018. Tracking vegetation phenology across diverse North American biomes using PhenoCam imagery. Sci. Data 5, 180028. https://doi.org/10.1038/sdata.2018.28.

Robson, T.M., Rasztovits, E., Aphalo, P.J., Alia, R., Aranda, I., 2013. Flushing phenology and fitness of European beech (*Fagus sylvatica* L.) provenances from a trial in La Rioja, Spain, segregate according to their climate of origin. Agric. For. Meteorol. 180, 76–85.

Rozas, V., 2003. Regeneration patterns, dendroecology, and forest-use history in an old-growth beech-oak lowland forest in Northern Spain. For. Ecol. Manage. 182, 175–194.

Rozas, V., Camarero, J.J., Sangüesa-Barreda, G., Souto, M., García-González, I., 2015. Summer drought and ENSO-related cloudiness distinctly drive *Fagus sylvatica* growth near the species rear-edge in northern Spain. Agric. For. Meteorol. 201, 153–164.

Rubtsov, V.V., Utkina, I.A., 2008. Adaptatsionnye reaktsii duba na defoliatsiyu (Adaptive Reaction of Oak on Defoliation). Grif i K, Moscow.

Sakai, A., Larcher, W., 1987. Frost Survival of Plants, Responses and Adaptation to Freezing Stress. Springer, New York.

San-Miguel-Ayanz, J., De Rigo, D., Caudullo, G., Houston Durrant, T., Mauri, A. (Eds.), 2016. European Atlas of Forest Tree Species. Publication Office of the European Union, Luxembourg.

Sánchez-Gómez, D., Robson, T.M., Gasco, A., Gil-Pelegrin, E., Aranda, I., 2013. Differences in the leaf functional traits of six beech (*Fagus sylvatica* L.) populations are reflected in their response to water limitation. Environ. Exp. Bot. 87, 110–119.

Sangüesa-Barreda, G., Camarero, J.J., Oliva, J., Montes, F., Gazol, A., 2015. Past logging, drought and pathogens interact and contribute to forest dieback. Agric. For. Meteorol. 208, 85–94.

Schweingruber, F.H., Eckstein, D., Serre-Bachet, F., Bräker, O.U., 1990. Identification, presentation and interpretation of event years and pointer years in dendrochronology. Dendrochronologia 8, 9–38.

Serra-Maluquer, X., Gazol, A., Sangüesa-Barreda, G., Sánchez-Salguero, R., Rozas, V., Colangelo, M., Gutiérrez, E., Camarero, J.J., 2019. Geographically structured growth decline of rear-edge Iberian *Fagus sylvatica* forests after the 1980s shift toward a warmer climate. Ecosystems. https://doi.org/10.1007/s10021-019-00339-z.

Serrano-Notivoli, R., Beguería, S., Saz Sánchez, M.A., et al., 2017a. SPREAD: a high-resolution daily gridded precipitation dataset for Spain—an extreme events frequency and intensity overview. Earth Syst. Sci. Data 9, 721–738.

Serrano-Notivoli, R., De Luis, M., Beguería, S., 2017b. An R package for daily precipitation climate series reconstruction. Environ. Model. Softw. 89, 190–195.

Serrano-Notivoli, R., Beguería, S., De Luis, M., 2019. STEAD: a high-resolution daily gridded temperature dataset for Spain. Earth Syst. Sci Dataessd-2019-52. in review, 2019.

Spulak, O., Martincova, J., 2015. The influence of the method of silver fir growing and nutrition on sprouting and chlorophyll fluorescence during spring. J. For. Sci. 61, 80–88.

Suvanto, S., Henttonen, H.M., Nöjd, P., Helama, S., Repo, T., Timonen, M., Mäkinen, H., 2017. Connecting potential frost damage events identified from meteorological

records to radial growth variation in Norway spruce and Scots pine. Trees-Struct. Funct. 31, 2023–2034.

Utkina, I., Rubtsov, V., 2017. Studies of phenological forms of pedunculate oak. Contemp. Probl. Ecol. 10, 804–811.

van der Maaten-Theunissen, M., van der Maaten, E., Bouriaud, O., 2015. pointRes: an R package to analyze pointer years and components of resilience. Dendrochronologia 35, 34–38.

Vanoni, M., Bugmann, H., Nötzli, M., Bigler, C., 2016. Drought and frost contribute to abrupt growth decreases before tree mortality in nine temperate tree species. For. Ecol. Manage. 382, 51–63.

Vicente-Serrano, Beguería, S., López-Moreno, J.I., 2010. A Multi-scalar drought index sensitive to global warming: the standardized precipitation evapotranspiration index – SPEI. J. Clim. 23, 1696–1718.

Vicente-Serrano, S.M., Gouveia, C., Camarero, J.J., Beguería, S., Trigo, R., López-Moreno, J.I., et al., 2013. Response of vegetation to drought time-scales across global land biomes. Proc. Natl. Acad. Sci. U. S. A. 110, 52–57.

Vitasse, Y., Rebetez, M., 2018. Unprecedented risk of spring frost damage in Switzerland and Germany in 2017. Climate 233–246 Ch. 149.

Vitasse, Y., Schneider, L., Rixen, C., Christen, D., Rebetez, M., 2018. Increase in the risk of

exposure of forest and fruit trees to spring frosts at higher elevations in Switzerland over the last four decades. Agric. For. Meteorol. 248, 60–69.

Vitasse, Y., Lenz, A., Hoch, G., Körner, C., Piper, F., 2014a. Earlier leaf-out rather than difference in freezing resistance puts juvenile trees at greater risk of damage than adult trees. J. Ecol. 102, 981–988.

Vitasse, Y., Lenz, A., Körner, C., 2014b. The interaction between freezing tolerance and phenology in temperate deciduous trees. Front. Plant Sci. 5, 541.

Vitra, A., Lenz, A., Vitasse, Y., 2017. Frost hardening and dehardening potential in temperate trees from winter to budburst. New Phytol. 216, 113–123.

Weigel, R., Muffler, L., Klisz, M., Kreyling, J., van der Maaten-Theunissen, M., Wilmking, M., van der Maaten, E., 2018. Winter matters: sensitivity to winter climate and cold events increases towards the cold distribution margin of European beech (*Fagus sylvatica* L.). J. Biogeogr. 45, 2779–2790. https://doi.org/10.1111/jbi.13444.

Zohner, C.M., Rockinger, A., Renner, S.S., 2019. Increased autumn productivity permits temperate trees to compensate for spring frost damage. New Phytol. 221, 789–795.

Zuur, A.F., Ieno, E.N., Walker, N., Saveliev, A.A., Smith, G.M., 2009. Mixed Effects Models and Extensions in Ecology with R. Springer.

Zuur, A.F., Ieno, E.N., Elphick, C.S., 2010. A protocol for data exploration to avoid common statistical problems. Methods Ecol. Evol. 1, 3–14.